matic dark-state structure (2). $|F_{extrapolated}|$ values were calculated by linear extrapolation from $|F_{dark}|$ and $|F_{photostationary}|$, by assuming equal occupancies of dark and bleached conformers in the photostationary state $|F_{extrapolated}| = 2 \times (|F_{photostationary}| - |F_{dark}|) + |F_{dark}|$. To enable structural changes and reduce model bias, we used the slowcool simulated annealing protocol in XPLOR with a 10-fold increased weighting ratio (W_A) (25) between x-ray and stereochemical terms. The resulting coordinates of the 10 selected residues were combined with monochromatic dark-state coordinates, as alternative conformers representing the bleached structural state. Positional and *B*-factor refinement of the combined coordinates against $|F_{photostationary}|$, again restricting movement to the 10 selected residues of the bleached structure, gave an *R* factor of 23.8%. The higher *R* factor of the selected-atom refinement is due to structural changes away from the active site that reflect systematic errors or changes in experimental conditions between the monochromatic (2) and Laue data sets. Those changes were also observed in refinement of dark-state coordinates against dark-state Laue data (*R* factor 20.7%) (27). Therefore, compared to the previously published dark-state structure (2), coordinates from the selected-atom refinement better indicate changes due solely to photobleaching and were used for all figures.

21. R. A. Mathies, S. W. Lin, J. B. Ames, W. T. Pollard, *Annu. Rev. Biophys. Biophys. Chem.* **20**, 491 (1991); Q. Wang, R. W. Schoenlein, L. A. Peteneau, R. A. Mathies, C. V. Shank, *Science* **266**, 422 (1994).
22. D. W. J. Cruickshank, J. R. Helliwell, L. N. Johnson, *Philos. Trans. R. Soc. London* **340**, 167 (1992).
23. E. D. Getzoff *et al.*, *Nucl. Instrum. Methods Phys. Res.* **79**, 249 (1994).
24. J. R. Helliwell *et al.*, *J. Appl. Crystallogr.* **22**, 483 (1989); T. J. Greenhough and A. K. Shrive, *ibid.* **27**, 111 (1994); J. W. Campbell, *ibid.* **28**, 228 (1995).
25. A. T. Brünger, J. Kuriyan, M. Karplus, *Science* **235**, 458 (1987); A. T. Brünger, A. Krukowski, J. W. Erickson, *Acta Crystallogr. A* **46**, 585 (1990).
26. D. E. McRee, *J. Mol. Graph.* **10**, 44 (1992); D. E. McRee, *Practical Protein Crystallography* (Academic Press, San Diego, CA, 1993).
27. U. K. Genick *et al.*, unpublished data.
28. C. Upson *et al.*, *IEEE Comput. Graph. Appl.* **9**, 30 (1989).
29. A. Nicholls and B. Honig, *J. Comput. Chem.* **12**, 435 (1991); A. Nicholls, K. A. Sharp, B. Honig, *DelPhi* (Department of Biochemistry and Molecular Biophysics, Columbia University, New York, NY, 1990).
30. A. D. MacKerell *et al.*, *FASEB J.* **6**, A143 (1992); A. D. MacKerell Jr. *et al.*, in preparation.
31. U. K. Genick *et al.*, *Biochemistry* **36**, 8 (1997).
32. We thank E. Blum, Y. Chen, A. LeGrand, H. E. Parge, and G. Shea-McCarthy for assistance in designing and constructing apparatus for these experiments and for help with data collection at NSLS, Brookhaven National Laboratory, and previous runs at CHESS, Cornell University; T. Greenhough for help with the Daresbury Laue program suite; J. A. Tainer and M. Baca for valuable discussions; and M. E. Pique for help with AVS figures. Coordinates for the PYP bleached intermediate have been deposited in the Protein Data Bank (accession number 2pyp). Supported by grants from NIH (GM37684 to E.D.G.; GM36452 and RR07707 to K.M.) and the W. M. Keck Foundation (M. Makinen and K.M.), and fellowships from NIH (NRSA GM15820 to G.E.O.B.) and Boehringer Ingelheim Fonds (U.K.G.).

26 June 1996; accepted 26 December 1996

PTG, a Protein Phosphatase 1–Binding Protein with a Role in Glycogen Metabolism

John A. Printen,* Matthew J. Brady,* Alan R. Saltiel†

Protein dephosphorylation by phosphatase PP1 plays a central role in mediating the effects of insulin on glucose and lipid metabolism. A PP1C-targeting protein expressed in 3T3-L1 adipocytes (called PTG, for protein targeting to glycogen) was cloned and characterized. PTG was expressed predominantly in insulin-sensitive tissues. In addition to binding and localizing PP1C to glycogen, PTG formed complexes with phosphorylase kinase, phosphorylase a, and glycogen synthase, the primary enzymes involved in the hormonal regulation of glycogen metabolism. Overexpression of PTG markedly increased basal and insulin-stimulated glycogen synthesis in Chinese hamster ovary cells overexpressing the insulin receptor, which do not express endogenous PTG. These results suggest that PTG is critical for glycogen metabolism, possibly functioning as a molecular scaffold.

The critical role of protein phosphorylation in the regulation of glucose and lipid metabolism has been recognized since the pioneering work of Krebs and Fischer in the 1950s (*1*). Insulin modulates many of the metabolic rate–limiting enzymes by promoting their net dephosphorylation, due to the activation of the type 1 serine-threonine protein phosphatase 1 (PP1) (*2*). Although the signaling pathways linking the insulin receptor to PP1 activation remain uncertain (*3*), the catalytic subunit of PP1 (PP1C) is thought to be maintained at discrete cellular locations in order to ensure the specificity of protein dephosphorylation produced by insulin (*4*). In mammals, two tissue-specific proteins have been identified that target PP1C to glycogen. RG1 encodes a protein product of 124 kD that is present in both heart and skeletal muscle (*5*). GL encodes a 33-kD glycogen and PP1C-binding subunit expressed exclusively in liver (*6*). Although phosphorylation of RG1 by the mitogen-activated protein kinase pathway was implicated in the regulation of PP1 activity (*7*), numerous studies have demonstrated that this phosphorylation cascade is neither necessary nor sufficient for the regulation of glycogen synthesis by insulin (*8*, *9*).

We used 3T3-L1 adipocytes, which are highly responsive to insulin, to identify PP1C-binding proteins that might be involved in insulin-mediated regulation of glycogen metabolism. A 3T3-L1 adipocyte cDNA library (*10*) fused to the Gal4p transcriptional activation domain was screened for proteins that interact with a Gal4p-PP1C DNA-binding domain fusion (*11*). Library plasmids expressing interacting proteins were identified by the ability to induce transcription of the integrated GAL1-lacZ reporter. One class of interacting cDNAs, typified by clone B1-1, consistently gave the highest levels of β-galactosidase (β-Gal) activity when plated on X-Gal–containing media. Partial DNA sequence from the GAL4 fusion junction followed by a BLAST search revealed that the cDNA contained in clone B1-1 was homologous to previously cloned PP1C glycogen-localizing subunits. Sequencing of an additional clone (B2-2) from the same class provided a probable translational initiation site (*12*). The PP1C-interacting cDNA contained in clones B1-1 and B2-2 was named PTG (protein targeting to glycogen).

PTG has amino acid sequence similarity to known glycogen-binding subunits of PP1C (Fig. 1). PTG is most similar to G_L (42% identity, 60% similarity), with less similarity to the skeletal muscle protein RG1 (26% identity, 49% similarity) and the yeast glycogen-binding subunit Gac1 (27% identity, 50% similarity) (*13*). The phosphorylation sites in RG1 that have been implicated in hormonal control of PP1C activity (*7*) are not conserved in PTG.

Northern (RNA) analysis of rat tissue revealed a PTG transcript of 3.0 kb expressed in all tissues except testis, being most abundant in skeletal muscle, liver, and heart. The 3.0-kb PTG transcript was also detected when 3T3-L1 fibroblasts were induced to differentiate into adipocytes (*14*), a transition correlated with a substantial increase in insulin sensitivity, including the stimulation of glycogen synthesis (*15*).

To determine whether PTG binds simultaneously to PP1C and glycogen, we evaluated their association in intact cells. A FLAG epitope–tagged PTG construct (pF-PTG) (*16*) was transiently transfected into Chinese hamster ovary cells overexpressing the insulin receptor (CHO-IR) (*17*), followed by immunoprecipitation with antibodies to FLAG (anti-FLAG) (*18*) and sub-

J. A. Printen and A. R. Saltiel, Department of Physiology, University of Michigan School of Medicine, Ann Arbor, MI 48109, and Department of Cell Biology, Parke-Davis Pharmaceutical Research Division, Warner-Lambert Company, Ann Arbor, MI 48105, USA.
M. J. Brady, Department of Cell Biology, Parke-Davis Pharmaceutical Research Division, Warner-Lambert Company, Ann Arbor, MI 48105, USA.

*These authors contributed equally to this work.
†To whom correspondence should be addressed.

sequent immunoblotting with anti-PP1C. PP1C was coimmunoprecipitated from cell lysates with anti–FLAG-PTG (Fig. 2A), demonstrating direct association of PP1C with PTG. To determine the subcellular localization of PTG, we fractionated similarly transfected CHO-IR cells by differential centrifugation (*19*) followed by SDS–polyacrylamide gel electrophoresis (PAGE) and immunoblotting with anti-FLAG. FLAG-PTG in the 14,000*g* supernatant localized exclusively to the glycogen-enriched cell fraction (Fig. 2B). Immunoblotting of these same samples with anti-PP1C showed that overexpression of FLAG-PTG in these cells caused a marked redistribution of PP1C from the cytosol into the glycogen pellet (Fig. 2C). Thus, PTG can simultaneously and specifically associate with both PP1C and glycogen in intact cells.

To determine whether PTG is involved in the localization of glycogen-metabolizing enzymes and of the kinases and phosphatases involved in their regulation, we performed in vitro binding assays with a glutathione-S-transferase (GST)–PTG fusion protein (*20*). Glutathione-Sepharose–bound GST-PTG was incubated with purified enzymes and assayed for the ability to form stable complexes (*21*). Glycogen synthase activity (Fig. 2D) and phosphorylase a (Fig. 2E) were specifically associated with GST-PTG, but not with an unrelated fusion protein, GST-PTP1B. Phosphorylase kinase, which converts phosphorylase from the inactive b form to the active a form, was also tested for PTG-binding activity. Calcium-stimulated phosphorylase kinase activity (*22*) was specifically associated with GST-PTG, but not with GST-PTP1B (Fig. 2F).

To characterize the specificity of these protein-protein interactions in the intact cell, we precipitated these enzymes from 3T3-L1 lysates with immobilized GST-PTG (*23*). The results summarized in Table 1 indicate that under identical conditions, PTG can form complexes with PP1C and phosphorylase kinase, but not with the type II serine-threonine phosphatase PP2A nor cyclic AMP (cAMP)–dependent protein

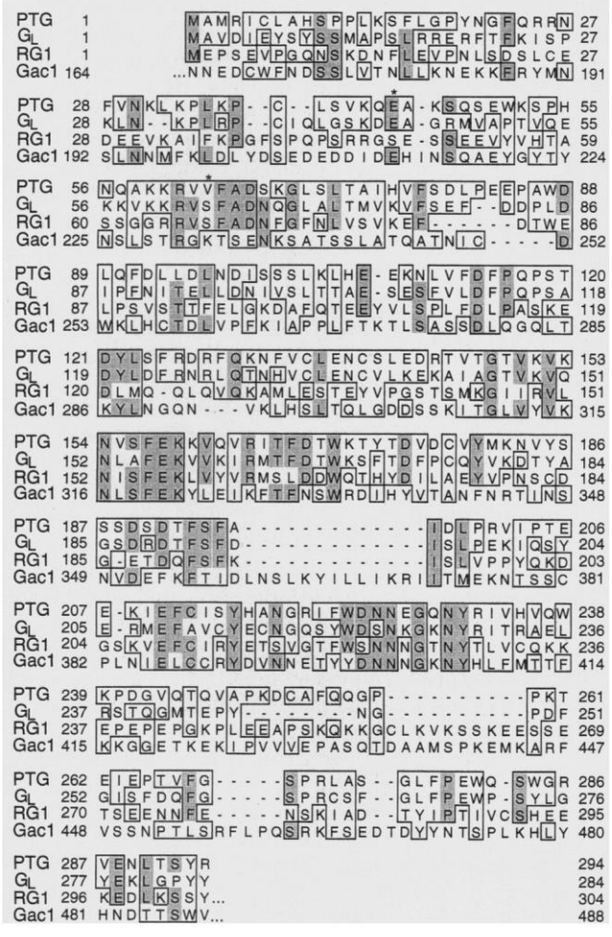

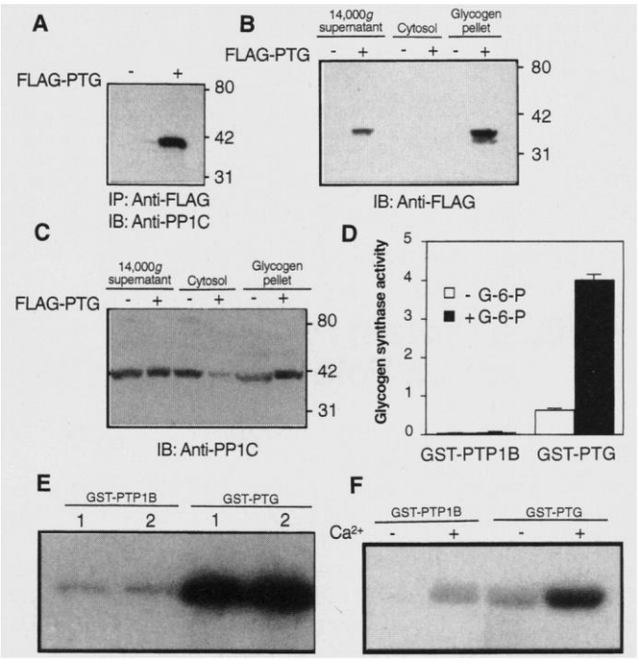

Fig. 1 (left). Sequence comparison of PTG with glycogen-localizing subunits of PP1C. The boxed regions represent areas of similarity, and the conserved residues are indicated by shading. Phosphorylation sites 1 and 2 of RG1 are indicated by asterisks. The nucleotide sequence of PTG has been deposited with GenBank (accession number U89924). **Fig. 2 (right).** PTG localizes PP1C to the glycogen-enriched pellet and binds glycogen-metabolizing enzymes. (**A**) PP1C binds PTG in vivo. pCI-neo–expressing FLAG-PTG (+) or lacZ (−) from the CMV promoter was transiently transfected into CHO-IR cells and immunoprecipitated from cell lysates with antibodies directed against the FLAG epitope. Precipitates were analyzed by SDS-PAGE, transferred to nitrocellulose, and blotted with polyclonal antibodies to PP1C. (**B**) PTG partitions to the glycogen pellet. Lysates from pFLAG-PTG–transfected (+) or mock-transfected (−) CHO-IR cells were fractionated by centrifugation into 14000*g* supernatant, cytosol, or glycogen pellet, and proteins were subjected to SDS-PAGE and immunoblotted with anti-FLAG. (**C**) PTG overexpression causes translocation of PP1C to the glycogen pellet. Lysates from pFLAG-PTG–transfected (+) or untransfected (−) CHO-IR cells were fractionated by centrifugation and immunoblotted as in (B) to determine relative levels of PP1C contained in the various fractions. (**D**) PTG binds glycogen synthase. GST-PTG (100 μl) bound to glutathione-Sepharose beads was resuspended in 725 μl of glycogen synthase buffer [50 mM Hepes (pH 7.8), 100 mM NaF, 10 mM EDTA] plus 25 μl of purified glycogen synthase, followed by incubation at 4°C for 1 hour with gentle mixing. The Sepharose beads were washed four times with glycogen synthase buffer and assayed for glycogen synthase activity (expressed as nanomoles of UDP-glucose incorporated per 15 min) (*21*). (**E**) PTG binds phosphorylase a. ^{32}P-labeled phosphorylase a (25 μg) was incubated with the indicated fusion protein immobilized to glutathione-Sepharose beads for 1 hour at 4°C in homogenization buffer, containing 0.1% BSA and 0.15 M NaCl, followed by washing four times with buffer before the addition of SDS sample buffer. Proteins were separated by SDS-PAGE, and the gel was exposed to film. Assays were performed in duplicate (1 and 2). (**F**) PTG binds phosphorylase kinase. Bacterially expressed GST-PTG (50 μl) bound to glutathione-Sepharose beads was incubated with 10 μg of purified phosphorylase kinase in homogenization buffer. Samples were incubated for 30 min at 4°C, washed four times with the same buffer, and assayed for phosphorylase kinase activity (*21*).

kinase (PKA), demonstrating the specificity of binding for both phosphatases and kinases to PTG. As seen in the in vitro binding assays, glycogen synthase from cell extracts could also efficiently bind to GST-PTG. Taken together, these results imply that PTG can complex with each of the key proteins involved in regulating glycogen metabolism, although it is unclear whether all of the glycogen-metabolizing enzymes are bound to a single PTG molecule or if individual binding sites are shared between one or more proteins.

Table 1. Enzymatic activity associated with immobilized GST-PTG fusion protein. Immobilized PTG or PTP-1B GST-fusion proteins were incubated with cell extracts prepared from 3T3-L1 adipocytes, followed by extensive washing to remove nonspecifically bound proteins. Enzymatic activity was determined as described (*23*). Phosphatase activity is expressed as picomoles of PO_4 released per minute, kinase activity as picomoles of PO_4 incorporated per minute, and synthase activity as picomoles of UDP-glucose incorporated per minute. Results are expressed as means of triplicate determinations (± SD) and are representative of experiments that were repeated twice.

Enzyme	Activity	
	GST-PTG	GST–PTP-1B
PP1	1.15 ± 0.08	0.0 ± 0.05
PP2A	0.06 ± 0.04	0.10 ± 0.01
Phosphorylase kinase	0.42 ± 0.01	0.06 ± 0.0
PKA	0.07 ± 0.0	0.06 ± 0.01
Glycogen synthase	352 ± 4.9	46.1 ± 1.5

To determine whether insulin altered the ability of PTG to form protein complexes, we stimulated cells with insulin and assayed the protein-protein associations. Insulin treatment of CHO-IR cells expressing FLAG-PTG did not affect the formation of PP1C-PTG complexes (Fig. 3A). Moreover, PTG itself was not phosphorylated in CHO-IR cells or 3T3-L1 adipocytes in response to insulin and was not a substrate in vitro for PKA or other protein kinases in lysates from insulin-stimulated cells (*14*). Insulin also did not affect the association of PTG with glycogen synthase, although it did induce a downward shift in the electrophoretic mobility of glycogen synthase in these cells (Fig. 3B), indicating that the dephosphorylated, active form of the enzyme remained bound to PTG. Phosphorylase kinase activity could also be coimmunoprecipitated with PTG from 3T3-L1 adipocyte lysates (Fig. 3C). Although the amount of enzymatic activity found in these complexes was reduced in response to insulin, it is unclear whether this decrease is the result of inactivation of the enzyme by dephosphorylation or of decreased binding affinity for PTG. We were unable to detect phosphorylase protein in either 3T3-L1 or CHO-IR cells, and it remains uncertain whether PTG can bind this enzyme in vivo.

These findings prompted us to examine whether overexpression of PTG would increase basal or insulin-stimulated glycogen synthesis. CHO-IR cells express no detectable PTG transcript or protein and have a low basal rate of glycogen synthesis, which increases ~1.5- to 2-fold upon insulin treatment (Fig. 3D). Overexpression of PTG in the CHO-IR cells caused a sevenfold increase in the basal rate of glycogen synthesis. Exposure of these cells to insulin produced a further twofold increase, with total glycogen synthesis being increased over 10-fold. Thus, PTG overexpression not only can increase basal glycogen synthesis, but also can markedly increase maximally insulin-stimulated glycogen accumulation in a poorly responsive cell line to a level comparable to that observed in insulin target cells (*9*). However, because the sensitivity of these transfected cells to insulin remains unchanged, and because insulin does not appear to modulate either PP1C-PTG binding or PTG phosphorylation, PTG itself is not likely to be a direct target of insulin signaling.

PP1C is present in almost all tissue types, not only in insulin-responsive cells (*24*). In addition to its association with glycogen, PP1C is found in the nucleus, cytoplasm, and other cellular compartments and is critical in many aspects of hormone action and secretion (*25*). Despite its ubiquitous expression, numerous studies indicate that PP1 plays a key role in insulin action, particularly in the regulation of glucose and lipid metabolism. Moreover, insulin promotes the dephosphorylation of only a limited number of substrates in its target cells (*26*). Taken together, these observations indicate that mechanisms must exist for the compartmentalized regulation of protein dephosphorylation by insulin. PTG may fulfill an important role in this process, because it is expressed in insulin-responsive tissues. This protein may assemble glycogen synthase, phosphorylase a, phosphorylase kinase, and PP1C onto the glycogen particle, generating a metabolic module for the localized reception of the appropriate intracellular signals. It is likely that PTG is itself not a classical regulatory molecule in glycogen metabolism, but rather may serve as a molecular scaffold, allowing hormonal signals to specifically target the relevant glycogen-associated enzymes.

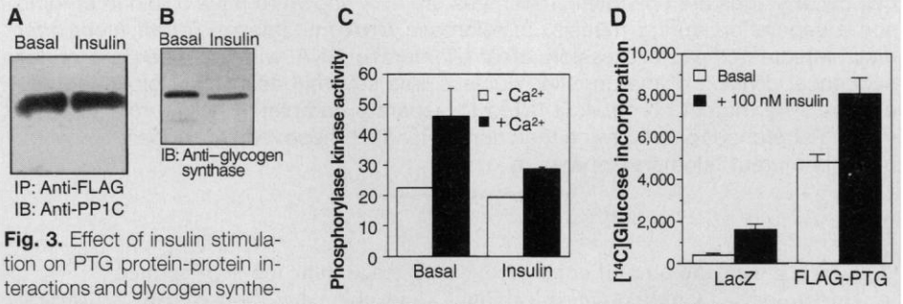

Fig. 3. Effect of insulin stimulation on PTG protein-protein interactions and glycogen synthesis. Insulin does not affect PTG binding to (**A**) PP1C, (**B**) glycogen synthase, or (**C**) phosphorylase kinase. (A) CHO-IR cells transiently transfected with pFLAG-PTG were serum-deprived for 3 hours before the addition of 100 nM insulin for 15 min. Cells were lysed in 400 μl of homogenization buffer, and FLAG-PTG was immunoprecipitated with anti-FLAG monoclonal antibody. Proteins were separated on a 4 to 20% SDS-polyacrylamide gel, transferred to nitrocellulose, and probed with anti-PP1C. (B) 3T3-L1 adipocytes were cultured and lysed as in (A). Lysates were immunoprecipitated with polyclonal antibodies raised against a bacterially expressed GST-PTG fusion protein, and immunoblots were probed with antibodies to glycogen synthase. (C) Endogenous PTG was immunoprecipitated from 3T3-L1 lysates treated as in (A), and PTG-associated phosphorylase kinase activity (expressed as picomoles PO_4 incorporated per minute) was determined (*21*). (**D**) Glycogen synthesis in CHO-IR cells overexpressing PTG. CHO-IR cells were grown to 40 to 50% confluency in six-well dishes and transiently transfected with pFLAG-PTG. Forty-eight hours after transfection, cells were serum-deprived for 3 hours, and glycogen accumulation in intact pFLAG-PTG– or lacZ-transfected cells, in the presence or absence of 100 nM insulin, was determined (*9*). Only 20% efficiency of transfection was obtained in these experiments, suggesting that the 10-fold increase in maximal glycogen synthesis by PTG is substantially underestimated. Results are expressed as means of triplicate determinations (±SD) and were repeated in two separate experiments.

REFERENCES AND NOTES

1. E. G. Krebs and E. H. Fischer, *Biochim. Biophys. Acta* **20**, 150 (1953).
2. P. Cohen, *Annu. Rev. Biochem.* **58**, 453 (1989).
3. A. R. Saltiel, *Am. J. Physiol.* **33**, E375 (1996).
4. M. J. Hubbard and P. Cohen, *Trends Biochem. Sci.* **18**, 172 (1993); D. Mochly-Rosen, *Science* **268**, 247 (1995).
5. P. M. Tang, J. A. Bondor, K. M. Swidenck, A. A. DePaoli-Roach, *J. Biol. Chem.* **266**, 15782 (1991).
6. M. J. Doherty, G. Moorhead, N. Morrice, P. Cohen, P. T. W. Cohen, *FEBS Lett.* **375**, 294 (1995).
7. A. Donella-Deana, A. Lavoinne, O. Marin, L. A. Pinna,

P. Cohen, *Biochem. Biophys. Acta* **1178**, 189 (1993); C. Sutherland, D. G. Campbell, P. Cohen, *Eur. J. Biochem.* **212**, 581 (1993); P. Dent *et al.*, *Nature* **348**, 302 (1990).
8. R. J. Wiese *et al.*, *J. Biol. Chem.* **270**, 3442 (1995); T. Lin and J. C. Lawrence Jr., *ibid.* **269**, 21255 (1994); L. J. Robinson, Z. F. Razzack, J. C. Lawrence, D. E. James, *ibid.* **268**, 26422 (1993).
9. D. F. Lazar *et al.*, *ibid.* **270**, 20801 (1995).
10. 3T3-L1 fibroblasts were induced to differentiate into adipocytes as described (*9*), and polyadenylated [poly(A$^+$)] mRNA was obtained with the Messenger RNA Isolation kit (Stratagene, La Jolla, CA). Poly(A$^+$) mRNA (5 μg) was used to synthesize cDNA with the Stratagene cDNA synthesis kit. cDNA fragments were then ligated unidirectionally into Eco RI–Xho I–digested pGAD-GH GAL4 activation domain plasmid (Clontech, Palo Alto, CA).
11. A Gal4p–DNA-binding domain (BD) fusion of PP1C was constructed by cloning the entire PP1α open reading frame, contained within a 1.0-kb Eco RI–Bam HI fragment, into the Eco RI–Bam HI sites of pGBT9 (Clontech), creating BD-PP1C. Strain Y190 was transformed first with BD-PP1C, Trp$^+$ prototrophs were selected, and then strain Y190 was transformed with 150 μg of 3T3 L1 adipocyte library DNA. Transformants were selected by plating cells on synthetic medium lacking tryptophan, leucine, and histidine (SD-Trp-Leu-His) and containing 25 mM 3-aminotriazole. Colonies that appeared after 5 days of incubation at 30°C were patched onto SD-Trp-Leu-His plates and then replica-plated onto M63GV-Trp-Leu-His media containing 5-bromo-4-chloro-3-indolylphosphate-β-D-galactopyranoside (X-Gal; Gibco-BRL) for preliminary determination of β-Gal activity. Of ~3.5×10^5 total transformants, 64 His$^+$ prototrophic colonies were recovered, of which 27 were β-Gal–positive.
12. M. Kozak, *J. Cell Biol.* **108**, 229 (1989).
13. J. M. Francois *et al.*, *EMBO J.* **11**, 87 (1992).
14. J. A. Printen, M. J. Brady, A. R. Saltiel, data not shown.
15. B. C. Reed, S. H. Kaufmann, J. C. Mackall, A. K. Student, M. D. Lane, *Proc. Natl. Acad. Sci. U.S.A.* **74**, 4876 (1977); C. S. Rubin, A. Hirsch, C. Fung, O. M. Rosen, *J. Biol. Chem.* **253**, 7570 (1978); A. G. de Herreros and M. J. Birnbaum, *ibid.* **264**, 19994 (1989).
16. The FLAG-epitope (NH_2-DYKDDDDK-COOH) was introduced into pCI-neo (Promega, Madison, WI) by ligating complementary oligonucleotides into Nhe I–Eco RI–digested vector. A 1.0-kb Eco RI fragment from clone B1-1 was cloned in-frame at the Eco RI site of the resulting plasmid, producing plasmid pFPTG. The FLAG-PTG fusion is expressed from the strong cytomegalovirus (CMV) enhancer-promoter.
17. S. B. Waters, K. Yamauchi, J. E. Pessin, *Mol. Cell. Biol.* **15**, 2791 (1995).
18. CHO-IR cells transfected with pFPTG were sonicated in PP1 homogenization buffer (*9*) and centrifuged at 14000*g* for 10 min at 4°C to remove nuclei and cell debris. FLAG-PTG was immunoprecipitated from the supernatant by incubation with 10 μg of anti-FLAG (Kodak, New Haven, CT) for 1 hour at 4°C. Immune complexes were precipitated by incubation with protein A/G–agarose for 1 hour at 4°C and washed four times with homogenization buffer before the addition of SDS–sample buffer. Immunoprecipitates and subcellular fractions were separated on SDS-polyacrylamide gels, transferred to nitrocellulose, and probed with either FLAG monoclonal antibody or with affinity-purified polyclonal antibody to PP1 .
19. CHO-IR cells were washed three times with ice-cold phosphate-buffered saline, scraped in homogenization buffer, and samples sonicated and centrifuged at 2500*g* to remove nuclei and unlysed cells. The postnuclear supernatant was removed and centrifuged for 15 min at 10,000*g* and 1 hour at 100,000*g* to pellet plasma membranes and glycogen pellets, respectively. The final supernatant was called cytosol.
20. A 1.0-kb Eco R1 fragment from clone B1-1, encoding residues 8 to 293 of PTG, was subcloned into the Eco R1 site of pGEX-5X-3 expression vector. The GST-PTG fusion protein was expressed in *Escherichia coli* BL21(DE3)LysS and purified by affinity chromatography on glutathione-Sepharose beads.
21. Glycogen synthase: 100 μl of GST-PTG or GST-PTP1B (20 μg) bound to glutathione-Sepharose beads was resuspended in 725 μl of glycogen synthase buffer [50 mM Hepes (pH 7.8), 100 mM NaF, 10 mM EDTA] plus 25 μl (0.1 U) of purified glycogen synthase (Sigma), followed by incubation at 4°C for 1 hour with gentle mixing. The Sepharose beads were washed four times with glycogen synthase buffer, brought to a final volume of 300 μl, and 50 μl assayed for glycogen synthase activity by measuring the incorporation of uridine 5′-diphosphate (UDP)–[^{14}C]glucose into glycogen, in the presence and absence of 10 mM glucose-6-phosphate. Phosphorylase: 50 μl of fusion protein beads were added to 750 μl of homogenization buffer containing 0.15 M NaCl, 0.1% bovine serum albumin (BSA), and 25 μg of ^{32}P-labeled phosphorylase a. The tubes were incubated at 4°C for 1 hour, washed four times with homogenization buffer, and proteins were separated by SDS-PAGE, followed by autoradiography. Phosphorylase kinase: Fusion protein beads (50 μl) were incubated with 10 μg of purified phosphorylase kinase (Gibco-BRL) in homogenization buffer plus 0.15 M NaCl and 0.1% BSA, incubated for 30 min at 4°C, and washed four times with the same buffer. Ten microliters of beads and 2 μg of phosphorylase b were assayed for 5 min at 37°C in 50 mM Hepes (pH 7.4), 10 mM $MgCl_2$, 1 μM okadaic acid, and 20 μM [γ-^{32}P]ATP (4000 cpm/pmol), in the absence (1 mM EGTA) or presence (0.5 mM) of Ca^{2+}. At the end of the incubation period SDS-sample buffer was added, proteins were separated by SDS-PAGE, and radiolabeled phosphorylase a was visualized by autoradiography and quantitated by scintillation counting.
22. E. G. Krebs *et al.*, *Biochemistry* **3**, 1022 (1964).
23. Glycogen synthase, phosphorylase kinase, and PKA assays: 3T3-L1 adipocytes were lysed in 1 ml of homogenization buffer and incubated with 25 μg of fusion protein immobilized on glutathione-Sepharose beads for 1 hour at 4°C. The beads were washed four times with homogenization buffer and assayed for bound glycogen synthase in the presence of glucose-6-phosphate (*9*). Phosphorylase kinase activity was determined as above (*21*). PKA activity was determined with bacterially expressed NH_2-terminal portion of RG1 (5 μg) in the presence and absence of 0.1 mM dibutyryl-cyclic AMP (dbcAMP). PP1 and PP2A: 3T3-L1 adipocytes were lysed in 1 ml of homogenization buffer and incubated as above with fusion protein. After extensive washing, the beads were assayed for phosphatase activity in the presence of 0, 3, and 500 nM okadaic acid. Activity loss between 0 and 3 nM is attributed to PP2A activity; loss between 3 and 500 nM is due to PP1 activity (*2*). Okadaic acid (500 nM) completely inhibited all phosphatase activity on the beads or in the starting extract.
24. H. Shima *et al.*, *Biochem. Biophys. Res. Commun.* **192**, 1289 (1993); H. Shima *et al.*, *ibid.* **194**, 930 (1993).
25. S. Shenolikar and A. C. Nairn, *Adv. Second Messenger Phosphoprotein Res.* **23**, 1 (1991); S. Shenolikar, *Annu. Rev. Cell Biol.* **10**, 55 (1994).
26. A. R. Saltiel, *FASEB J.* **8**, 1034 (1994).
27. We thank M. Chang for the pCI-neo/FLAG construct, A. Nairn for PP1α cDNA, and J. Lawrence for antibodies to PP1Cα and glycogen synthase.

10 September 1996; accepted 27 January 1997

Block in Anaphase Chromosome Separation Caused by a Telomerase Template Mutation

Karen E. Kirk,* Brian P. Harmon, Isabel K. Reichardt, John W. Sedat, Elizabeth H. Blackburn†

Telomeres are essential for chromosome stability, but their functions at specific cell-cycle stages are unknown. Telomeres are now shown to have a role in chromosome separation during mitosis. In telomeric DNA mutants of *Tetrahymena thermophila*, created by expression of a telomerase RNA with an altered template sequence, division of the germline nucleus was severely delayed or blocked in anaphase. The mutant chromatids failed to separate completely at the midzone, becoming stretched to up to twice their normal length. These results suggest a physical block in mutant telomere separation.

Telomeres "cap" the termini of eukaryotic chromosomes. Chromosomes lacking telomeres undergo fusion, degradation, and extremely high loss rates (*1*–*3*). However, there is little information on the mechanism by which telomeres ensure chromosome stability, or at what cell-cycle stage their job is performed.

In the ciliated protozoan *Tetrahymena thermophila* the transcriptionally active, polygenomic macronucleus divides amitotically, whereas the diploid germline micronucleus, with its chromosomal complement of five pairs of metacentric chromosomes, divides mitotically (*4*). The telomeric DNA tracts of the two nuclei have the same terminal GGGGTT repeat sequence, although the tracts are markedly different in overall length (*5*). Whereas macronuclear telomeres play a crucial role in amitotic macronuclear divisions (*6*), the function of micronuclear telomeres has not been examined. Micronuclear chromosomes are trancriptionally quiescent and mostly dispensable for vegeta-

K. E. Kirk, I. K. Reichardt, E. H. Blackburn, Department of Microbiology and Immunology, University of California, San Francisco, 513 Parnassus, Box 0414, San Francisco, CA 94143–0414, USA.
B. P. Harmon and J. W. Sedat, Department of Biochemistry and Biophysics, University of California, San Francisco, 513 Parnassus, Box 0554, San Francisco, CA 94143–0414, USA.

*Present address: Department of Biology, Lake Forest College, Lake Forest, IL 60045, USA.
†To whom correspondence should be addressed.